DE GRUYTER

Chemical Papers 70 (6) 669–684 (2016)
DOI: 10.1515/chempap-2016-0004

ORIGINAL PAPER

A practical approach to non-spectral interferences elimination in inductively coupled plasma optical emission spectrometry

Anna Krejčová*, Tomáš Černohorský, Lenka Bendakovská

Department of Environmental and Chemical Engineering, Faculty of Chemical Technology, University of Pardubice, Studentská 573, 532 10 Pardubice, Czech Republic

Received 10 August 2015; Revised 12 November 2015; Accepted 14 November 2015

Matrix effects and practical possibilities of reducing accompanying non-spectral interferences in inductively coupled plasma optical emission spectrometry (ICP-OES) were studied for microconcentric Micromist, concentric and V-groove nebulizers (VGN) coupled with two cyclonic spray chambers of different sizes. The effect of a wide scale of interferents and mixtures thereof in the concentration range of up to 2 mass % (Na, Ca, Ba, La, urea) or up to 20 vol. % (nitric acid) on the analysis of Cd, Cu, K, Mg, Mn, Pb and Zn was investigated in terms of their analytical recovery and Mg(II) 280.27 nm/Mg(I) 285.29 nm line intensity ratio. Recoveries of ionic lines were lower than those of atomic lines (37–102 %) depending on the matrix concentration. The Mg(II)/Mg(I) ratios were found to be 12–15 and they slightly decreased as the matrix load increased. Exceptional behavior of pure La matrix, steeply lowering the recoveries and Mg(II)/Mg(I) ratios was observed. A Micromist nebulizer coupled with a small inner volume spray chamber provided the highest recoveries (94–102 %), lowest matrix effects across the matrix loads and, compared to others, the least significant dependence without worsening of the analytical characteristics (recoveries, signal background ratios and the Mg(II)/Mg(I) ratios) across the studied matrices.

Keywords: ICP-OES, matrix effect, microconcentric Micromist nebulizer, spray chamber

Introduction

Matrix effects have been discussed in a number of articles from many different points of view. Attention has been often focused on the individual matrix components or mixtures thereof in analyzed samples and their effect on the final outcome analysis. Matrix effects have been frequently discussed in regard to physical properties of a nebulized solution or shifts in excitation processes. Many authors have focused on the mechanisms of matrix effects at different experimental arrangements or working conditions.

Investigations of non-spectral interferences often deal with the so-called easily ionized elements (EIEs) with low ionization potential, i.e. alkaline and alkaline earth elements often present in biological and environmental samples (Todolí et al., 2002). Representing EIEs, Li, Na, K, Ca, Mg, Rb, Ba and La have been used in the matrix effect studies individually or in mixtures in concentrations up to 20 g L^{-1} (Todolí et al., 2002, 2004; Stepan et al., 2001; Maestre et al., 2002; Chan & Hieftje, 2008a; Iglésias et al., 2004; Chan & Hieftje, 2008b; Bauer & Broekaert, 2007; Cano et al., 2002; Ardini et al., 2012; Borkowska-Burnecka et al., 2006; Aguirre et al., 2010, Krejčová et al., 2001; Krejčová & Černohorský, 2003). Na, K, Rb, and Ba are elements with low first and second (Ba) ionization potentials (Bauer & Broekaert, 2007; Aguirre et al., 2010); La represents a line-rich element (Chan & Hieftje, 2008a). A wide range of inorganic and organic acids (from storage and pretreatment steps) alone and in mixtures has been tested (Todolí & Mermet, 1999). The effects of nitric acid (Stewart & Olesik, 1998), nitric and sulfuric acids, individually and in a mixture

*Corresponding author, e-mail: anna.krejcova@upce.cz

(Elgersma et al., 2000), as well as of nitric, hydrochloric, sulfuric and perchloric acids, separately or mixed (5–80 vol. %) (Grotti et al., 2002), nitric and acetic acids (de Gois et al., 2012), citric, tartaric and dipiclonic acids (Rončević & Pitarević Svedružić, 2012) and acetic, citric, hydrochloric, oxalic, nitric, perchloric and tartaric acids (Packer & Mattiazzo, 2007) have been studied. Mixtures of salts, acids and other inorganic and organic compounds have also been studied: acetic acid and sodium hydroxide (de Gois et al., 2012), nitric and acetic acids with sodium (Todolí et al., 2004), nitric acid, sodium and calcium (Stepan et al., 2001), nitric acid, chromium and carbon (Silva et al., 2002), mixtures of acids, EIEs and organic compounds (Paredes et al., 2006; Krejčová et al., 2001; Krejčová & Černohorský, 2003), lithium, copper and zinc matrix (Lehn et al., 2003), and carbon (Silva et al., 2002; Lehn et al., 2003).

Transport-related interferences originate from differences in the viscosity, volatility, density or surface tension of the samples and calibration standards. Matrix components influence the characteristics of tertiary aerosols and of the entire mass of the analyte moving into the plasma. They induce shifts in excitation mechanisms, plasma thermal characteristics, excitation efficiencies and in spatial distribution of emitted radiation (plasma-related effects) (Todolí et al., 2002; Mora et al., 2003; Dubuisson et al., 1998; Tripković & Holclajtner-Antunović, 1993).

Instrumental aspects and variables influencing aerosol generation and transport have been discussed. The spray chamber design plays a key role in the intensity of the matrix effects, particularly of the characteristics of the spatial emission profiles. For the reduction of interferences, low volume cyclonic spray chambers seem to be beneficial (Todolí et al., 2002, 2004; Maestre et al., 2002; Ardini et al., 2012; Packer & Mattiazzo, 2007; Benzo et al., 2009). Pneumatic concentric, cross flow and ultrasonic nebulizers are almost universally used as ICP-OES sample introduction systems. These nebulizers are efficient if operated at the solution uptake rates in the range of 0.5–3 mL min^{-1} (Elgersma et al., 2000), but their design is not optimized for rates under 1 mL min^{-1} (Todolí et al., 1999). In addition to the geometric arrangement, a critical parameter is the nebulizer liquid flow (Bauer & Broekaert, 2007; Todolí et al., 1999, 2004; Borkowska-Burnecka et al., 2006; Aguirre et al., 2010; Todolí & Mermet, 1999; Dubuisson et al., 1998; Maestre et al., 2004; Vanhaecke et al., 1996; Matusiewicz et al., 2007).

Analysis of small volumes is enabled by micronebulizers which are reported to be extremely sensitive to the interferences from the saline matrix but, on the other hand, more effective than conventional pneumatic nebulizers. Studies dealing with micronebulizers are principally devoted to the physical characteristics of the produced aerosol. There is an evident lack of works addressing the relationship between the composition of the matrix and its analytical performance. Maestre et al. (2004) characterized the behavior of five pneumatic micronebulizers and two spray chambers of various volumes at the liquid flows of 0.017–0.140 mL min^{-1} using certified reference materials. The nebulizer design did not have a relevant effect on the recovery, which confirmed that the spray chamber plays an important role concerning non-spectroscopic interferences. Performance of cross-flow (1.3 mL min^{-1}), ultrasonic (0.7 mL min^{-1}), Meinhard (0.4 mL min^{-1}) and Micromist (MMN; 0.02 mL min^{-1}) nebulizers was compared as to their efficiency in minimizing the spectral and non-spectral effects of acetic acid extracts. Lower non-spectral interferences were observed when using MMN than the other nebulizers (de Gois et al., 2012). Todolí et al. (1999) compared the high-efficiency nebulizer (HEN), the microconcentric nebulizer and MMN with a conventional pneumatic concentric nebulizer working at low liquid flow rates in ICP-OES. Physical characteristics of nebulized sample were followed. The micronebulizers provided finer primary aerosols, higher solution transport rates through the spray chamber and higher sensitivities than the conventional pneumatic concentric nebulizer. HEN provided slightly lower limits of detection than the other two micronebulizers.

In some cases, conventional nebulizers are operated at lower sample uptake rates than usual. Elgersma et al. (2000) reported a home-made, conventional glass pneumatic and concentric nebulizer used for low sample consumption uptake rates of 0.05–0.2 mL min^{-1} with aerosol desolvation. Signal to background values, detection limits and interferences seemed to be dependent on the liquid flow over the range of measured rates. Interferences were reduced by choosing an appropriate aerosol temperature and lowering the liquid flow (Elgersma et al., 2000). HEN and MMN were compared with a conventional concentric pneumatic nebulizer (CCN) working at low liquid flow rates (in the range of 0.05–0.16 mL min^{-1}). The use of micronebulizers led to good results when the sample volume or the solution rate was the limiting factor of the analysis. CCN operated at several tens of microliters per minute reached analyte transport efficiencies of about 20 %, but the high dead volume limited its use for the analysis of very low liquid sample volumes (Todolí et al., 1999).

The objective of the present work was to study the matrix effects of Na, Ca, Ba, La urea and nitric acid in the sample, introduce configurations with MMN coupled with spray chambers of two sizes and to compare the results with those of the CCN and V-groove nebulizers. Influence of the matrix on the analyte intensities and detection limits as well as on the ion to atom line intensity ratios was examined. A relationship between the experimental arrangement and the analytical recoveries under various matrix loads was searched for.

Table 1. Working conditions for the ICP OES analysis used in the interference study

Parameter	Value	Parameter	Value
Power/W	1100	Working gas (Ar) purity/%	99.999
Observation height/mm	7.0	Plasma gas flow/(L min^{-1})	11
PMT[a]/V	600	Auxiliary gas flow/(L min^{-1})	0.6
Replicates	5	Nebulizer gas flow/(mL min^{-1})	0.65

Tested introduction system combinations

Spray chamber	Nebulizer type	Sample uptake rate/(mL min^{-1})
Inner volume 50 mL	Concentric pneumatic	1.5
Inner volume 50 mL	V-groove	1.5
Inner volume 50 mL	Micromist	0.3
Inner volume 30 mL	Micromist	0.3

a) PMT – photomultiplier voltage was 550 V for both Mg(I) 280.270 nm and Mg(II) 285.213 nm.

Table 2. Composition of solutions of interferents used in the study

Matrix composition				low			full
Percentage of "full" matrix	0	0.5	2.5	5	25	50	100
Na, Ca, Ba, La, urea/mass %	0	0.01	0.05	0.1	0.5	1	2
HNO_3/vol. %	0	1.7	3.3	10	13	17	20

Experimental

The analysis was carried out using a sequential, radially viewed ICP-OES Integra XL 2 (GBC, Braeside, Australia). CCN, MMN, VGN and two glass cyclonic spray chambers (SC – "small" chamber, volume of 25 mL, LC – "large" chamber, 50 mL) were employed (all Glass Expansion, West Melbourne, Australia). Working conditions and lines are summarized in Table 1.

Calibration standards and test solutions were prepared using commercially available standard solutions of Cd, Cu, K, Mg, Mn, Pb and Zn, all in the concentration of (1.000 ± 0.003) g L^{-1} (SCP, Baie D'Urfé, Canada). NaCl, $CaCl_2$, $BaCl_2$ and urea interferents were of purity "for analysis" (LachNer, Neratovice, Czech Republic). Purity of La_2O_3 was 99.9 % (Rare earth products, Beverly, USA). The 65 vol. % nitric acid used both as an interferent and as a standard stabilizer was of purity "for semiconductors" (LachNer, Neratovice, Czech Republic).

ICP-OES multi-element standards contained: (i) 1 mg L^{-1} of Cd, Cu, Mn, and Zn, 0.2 mg L^{-1} of Mg, 5 mg L^{-1} of Pb and 10 mg L^{-1} K, and; (ii) half concentrations as in the first case; (iii) fivefold diluted; (iv) tenfold diluted and; (v) twenty-fold diluted as in the first case. Seven sets of test solutions were prepared as summarized in Table 2. All standards and test solutions were stabilized with 1 mL of 65 vol. % of HNO_3 in 100 mL of the final volume.

Results and discussion

Experimental design – interferents, analytical lines and working conditions

Four combinations of nebulizers and spray chambers were evaluated: VGN + LC, CCN + LC, MMN + LC and MMN + SC. Interferents Na, Ca, Ba, La and urea (up to 2 mass %), nitric acid (up to 20 vol. % of HNO_3) were used individually or as mixtures thereof (Table 3). Na, Ba and La represent EIEs, Na and Ba have low first and Ba also second ionization potential. Na and Ca salts are frequently present in the sample matrix. HNO_3 is widely used for decomposition as well as for stabilization of samples. Urea represents organic matter in poorly or not decomposed samples.

Cd, Cr, Cu, Mg, Mn, Ni, Pb and Zn were employed because they are commonly monitored in various samples and they are the most interesting elements for environmental studies. Emission lines (Table 3) were selected to cover a range of excitation and ionization energies including "soft" (K) and "hard" (Cd, Zn) as well as atomic (Cd, Cu, Zn, K, Mg) and ionic (Cd, Cu, Mn, Pb, Mg) lines (Lide, 2003). The final selection of spectral lines was made with regard to the signal-to-background (SBR) ratios, accuracy and sensitivity using spectral libraries available in the ICP-OES software.

Because of the variety of used spectral lines, compromise instrumental conditions had to be determined. For this purpose, solutions containing 0.5

Table 3. Analytical figure of merit: limits of detection (LOD), repeatabilities (RSD) and recoveries (R) for the experimental arrangements tested

Nebulizer/ Spray chamber	Parameter	Matrix	Line/(nm)							
			Cd(I) 228.802	Cd(II) 214.438	Cu(I) 224.700	Cu(II) 324.754	Mn(II) 257.610	Zn(I) 213.856	Pb(II) 220.353	K(I) 766.490
MMN+SC	LOD/(μg L^{-1})	"zero"	0.95	0.93	1.4	1.5	0.33	0.53	17	41
		"full"	1.9	2.3	2.3	2.8	1.3	1.9	31	74
	R/%	"zero"	100	100	98.7	98.5	98.0	98.7	101	96.2
		"full"	85.3	77.2	83.9	80.8	69.5	85.9	72.7	81.8
	RSD/%	"zero"	0.862	0.881	1.20	1.12	1.20	1.01	1.21	1.08
		"full"	1.35	1.27	1.26	1.58	1.45	1.29	1.38	1.50
MMN+LC	LOD/(μg L^{-1})	"zero"	1.2	0.95	1.4	1.7	0.33	0.82	19	43
		"full"	2.2	2.4	2.4	2.8	2.3	1.8	33	73
	R/%	"zero"	101	99.7	99.8	98.0	100	98.2	101	99.4
		"full"	80.4	76.7	76.8	73.5	80.2	79.5	69.6	83.5
	RSD/%	"zero"	1.42	1.26	1.33	1.15	1.45	1.25	1.17	1.16
		"full"	1.28	1.52	1.53	1.24	1.55	1.90	1.68	1.47
CCN+LC	LOD/(μg L^{-1})	"zero"	0.92	0.77	1.2	1.6	0.27	0.22	16	41
		"full"	1.8	1.8	2.3	2.7	0.89	1.2	31	74
	R/%	"zero"	100	99.0	100	99.2	99.0	100	101	96.9
		"full"	76.2	60.4	64.2	75.4	49.5	67.2	56.6	75.5
	RSD/%	"zero"	0.740	0.745	0.919	0.814	0.888	1.27	0.983	0.917
		"full"	0.856	1.53	1.30	1.63	1.53	1.93	1.42	1.33
VGN+LC	LOD/(μg L^{-1})	"zero"	1.3	1.2	1.6	2.8	2.2	0.80	22	62
		"full"	2.4	2.6	2.8	3.9	3.7	2.1	39	89
	R/%	"zero"	99.6	98.4	101	102	98.9	99.8	102	101
		"full"	55.8	51.2	59.8	55.0	56.4	57.9	55.0	63.5
	RSD/%	"zero"	1.51	3.09	3.59	2.68	3.32	4.08	5.27	3.88
		"full"	2.36	4.33	2.74	1.50	3.18	3.22	2.07	5.34

CCN – Concentric, MMN – Micromist, VGN – V-groove nebulizers, LC – large spray chamber, SC – small spray chamber, "full" matrix: 2 mass % of Na, Ca, Ba, La, urea and 20 vol. % of HNO_3 for VGN-LC and CCN-LC and 1 mass % of Na, Ca, Ba, La, urea and 17 mass % of HNO_3 for MMN+SC/LC.

mg L^{-1} of Cd, Cu, Mn and Zn, 0.1 mg L^{-1} of Mg, 2.5 mg L^{-1} of Pb and 5 mg L^{-1} of K in water ("zero") and in the most concentrated mixed ("full") matrix were examined in order to obtain both the highest signal to background ratio (SBR) and the lowest detection limits (LOD, Table 1). Across the lines and combinations of the nebulizer/spray chamber, optimal observation heights were approx. 7.0 mm above the coil while the optimal powers were in the range of 950 W to 1150 W. Both compromise parameters were set based on the most frequent values (7.0 mm, 1100 W).

The pump speed affects the volume of the aerosol as well as the efficiency of nebulization; and it is important in regard to the sensitivity and precision of analysis. A high sample delivery rate can increase the formation of large aerosol droplets, which results in a higher background level and in repeatability deterioration. The nebulizer liquid flow (Q_L, sample volume flow in the nebulizer within a defined time) was followed in the range of 0.1–1 mL min^{-1} for MMN and in the range of 0.8–2.2 mL min^{-1} for CCN and VGN for the water solution ("zero" matrix) and the matrix solution of the above mentioned analytes. The "full" mixed matrix solution at flow rates higher than 0.8 mL min^{-1} caused a blockade at the MMN orifice; therefore, a less concentrated solution was used (1 mass % of Na, Ca, Ba, La, urea and 17 vol. % of HNO_3) in further experiments.

In Fig. 1a, the effect of the nebulizer liquid flow on the analytical signals of Cd(II) 214.438 nm ("hard", ionic line) for the "zero" matrix and matrix solutions is displayed for all instrumental arrangements. Similarly, in Fig. 1b, the same effect is presented for K(I) 766.490 nm ("soft", atomic line). An increase in the nebulizer liquid flow led to a continuous increase of the analyte's response in case of the "zero" matrix. The increase of the intensity at the beginning of the flow range studied was significant, then, it slowed down (MMN) and passed into almost a "plateau" (CCN, VGN). For the matrix solution, a very slow continuous increase of the response was observed for the MMN nebulizer connected with both spray chambers. A significant increase of the signal was noticed for the CCN and VGN nebulizers; then, it slowed down and began to decline gradually. These trends, demonstrated by the Cd(II) and K(I) lines (Figs. 1a and 1b), were observed across all the spectral lines regardless of their

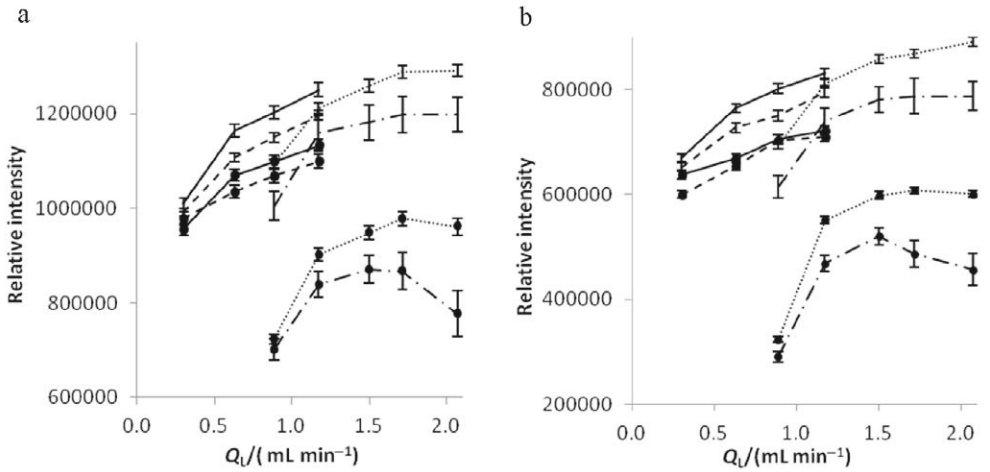

Fig. 1. ICP-OES intensities vs. nebulizer liquid flow, Q_L, for Cd 214.438 nm and K 760.490 nm: (a) Cd(II) 214.438 nm, and (b) K(I) 760.490 nm obtained for the "zero" matrix: MMN-SC ——, MMN-LC – – –, CCN-LC ·····, VGN-LC –·– ; and for the matrix of 1 mass % of Na, Ca, Ba, La, urea and 17 vol. % of HNO_3 MMN-SC —●—, MMN-LC – –●– –, CCN-LC ···●··, VGN-LC –·●–.

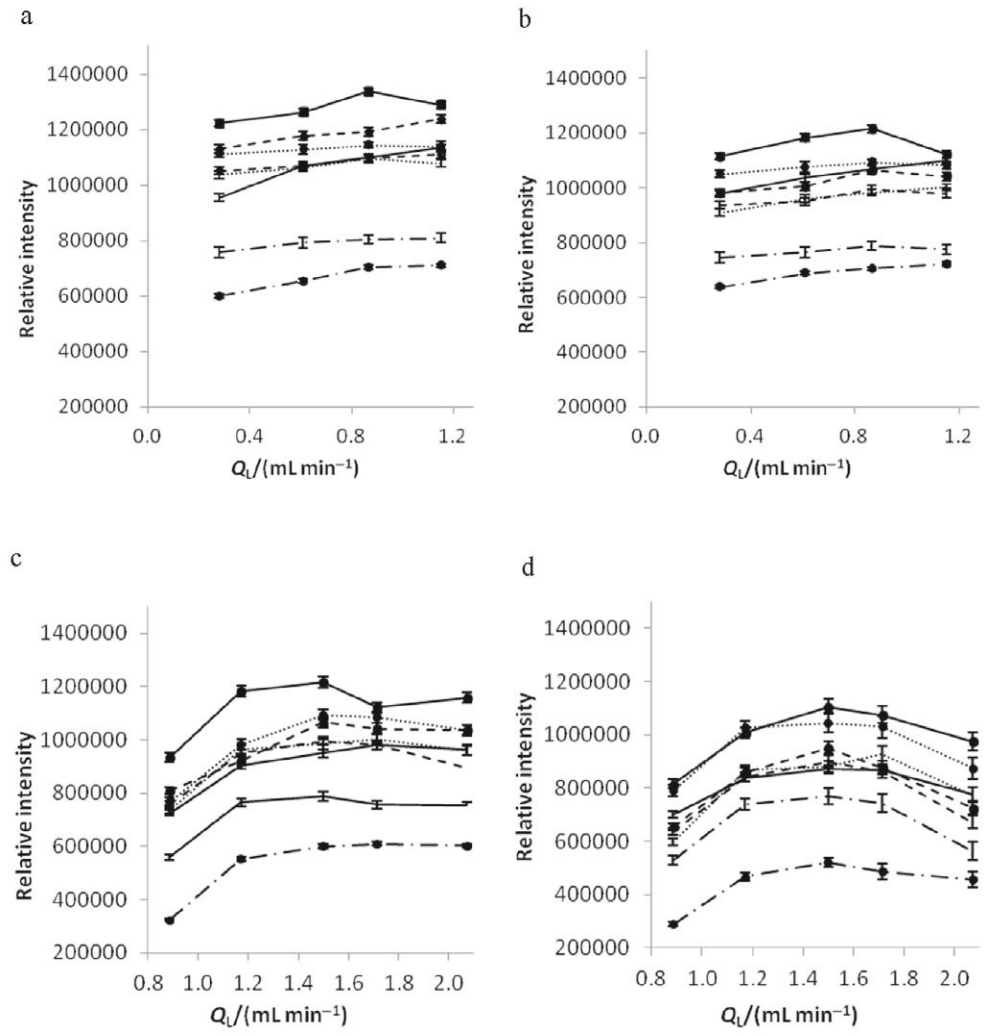

Fig. 2. ICP-OES intensities vs. nebulizer liquid flow, Q_L, for tested sample introduction systems. The curves were obtained for: (a) MMN-SC, (b) MMN-LC, (c) CCN-LC, (d) VGN-LC, and for the matrix of 1mass % of Na, Ca, Ba, La, urea and 17 vol. % of HNO_3 across the selected spectral lines: Cd II 214.438 ——, Cd I 228.802 —●—, Cu II 224.700 – – –, Cu I 324.754 – –●– –, Mn I 257.610 ·····, Zn I 213.856 ···●··, Pb II 220.353 –·–, K I 766.490 –·●–.

ionization energy. A little stronger signal decrease was observed in ionic lines, especially for the VGN nebulizer. For the matrix solution, the decrease of the signal was stronger for CCN and VGN than those observed for the MMN arrangements.

In Figs. 2a–2d, dependences of the signals of all spectral lines studied on Q_L are presented for all nebulizer arrangements and the matrix solution. A very similar behavior of all lines was revealed: for both MMN arrangements, a slight increase in the signals passing into a plateau was observed. For the CCN nebulizer, the increase in the intensity was steeper, then, it slowed down and resulted in a plateau. In case of VGN, at the flow rates of about 1.8–2.2 mL min^{-1}, the signals slowly decreased. There was an almost unrecognizable difference in the behavior of the atomic and ionic lines. The effect of the nebulizer flow rate was rather dependent on the nebulizers used. This phenomenon has been already discussed in literature, especially for micronebulizers used both in ICP-OES and in ICP-MS; contradictory results depending on the nebulizer type and the range of flow rates were obtained (Todolí et al., 1999; Todolí & Mermet, 2001; Becker & Dietze, 1999).

With the increased flow rate, a noticeable fluctuation in the formed amount of aerosol was observed and the signal repeatability decreased for the VGN nebulizer. The final sample uptake rate was set as a compromise respecting also the nebulizer producer recommendation. The final values selected were 0.3 mL min^{-1} and 1.5 mL min^{-1} for MMN and both CCN and VGN, respectively.

Analytical figures of merit

LODs expressed as the concentration related to the triple of the standard deviation of noise at the point of background correction are summarized (Table 3) together with the typical repeatabilities (relative standard deviations, RSD) for ten replicates of the middle calibration standard for the "zero" and "full" matrix. As shown in Table 3, LODs for the "full" matrix compared to the "zero" one were 1.6–2.1 time higher. The deterioration of LODs in the presence of matrix is consistent with other studies (Cano et al., 2002; Borkowska-Burnecka et al., 2006; de Gois et al., 2012; Silva et al., 2002). The differences were slightly higher for the ionic than for the atomic lines. In comparison with CCN, values obtained for VGN were 1.3–8.2 times higher, which is in agreement with literature (Borkowska-Burnecka et al., 2006). LODs for CCN and both MMN arrangements were almost comparable, similarly as presented by de Gois et al. (2012). On the other hand, the half detection limit values were presented for various micronebulizers and they were compared to those obtained for a pneumatic one (Todolí et al., 1999). LODs for MMN-SC were slightly lower than those for MMN-LC. Also, quite different LODs for various nebulizers obviously depending on the transport efficiency, type of the spray chamber used and the final aerosol load to the plasma were presented (Cano et al., 2002; Borkowska-Burnecka et al., 2006; Elgersma et al., 2000; Packer & Mattiazzo, 2007; Silva et al., 2002). Relating to the worse LODs obtained for the matrix, a decrease of SBRs was observed in the presence of the "full" matrix, approximately by 20–40 % (Fig. S1, in Supplementary data).

Uncertainties were expressed as RSDs (Table 2); higher RSDs were obtained for the "full" than for the "zero" matrix. For VGN, RSDs were found to be 1.5–5.3 % for the "zero" and 1.5–5.5 % for the "full" matrix. RSDs for the other three experimental arrangements were slightly lower, 0.7–1.5 % and 0.9–1.9 % for the "zero" and "full" matrix, respectively. Deterioration of RSDs in the presence of matrix was reported depending on the sample introduction system arrangements (Cano et al., 2002; Aguirre et al., 2010; Elgersma et al., 2000; Packer & Mattiazzo, 2007).

To complete the analytical figures of merit, recoveries are summarized in Table 3 for the "zero" and "full" matrix. There is an evident effect of the presence of matrix components, which together in a mixture cause a decrease of analytical signals across the studied spectral lines. This phenomenon is discussed in detail in the following chapter.

Recovery for the tested sample introduction systems

Matrix effects were examined considering a wide range of interferents and concentrations. The "full" matrix is an extreme situation, rather rare in laboratory routine and even in literature (Todolí et al., 2002, 2004; Stepan et al., 2001; Maestre et al., 2002; Chan & Hieftje, 2008a; Iglésias et al., 2004; Chan & Hieftje, 2008b; Bauer & Broekaert, 2007; Cano et al., 2002; Ardini et al., 2012; Borkowska-Burnecka et al., 2006; Aguirre et al., 2010). This matrix composition approaches the upper instrumental limit of salts in analyzed solutions (30 %) recommended by the manufacturer. The "low" matrix (Table 2) contains only 5 % of this limit and is more realistic when considering the samples routinely analyzed. The matrix effect is relatively intensive for all spectral lines in the study (Figs. 3–10).

For both, single and mixed matrices, a decrease of the analytical signals was observed, which was a little more pronounced for ionic than for atomic lines. This is in agreement with literature (Borkowska-Burnecka et al., 2006), where both negative and positive changes of line intensities were observed. Only suppression of intensities determined in our study can correspond with the robust plasma conditions in which the experiment was carried out (as discussed and confirmed in the next chapter "Mg ionic-to-atomic (Mg(II)/Mg(I) intensity ratios"). Stepan et al. (2001) described the

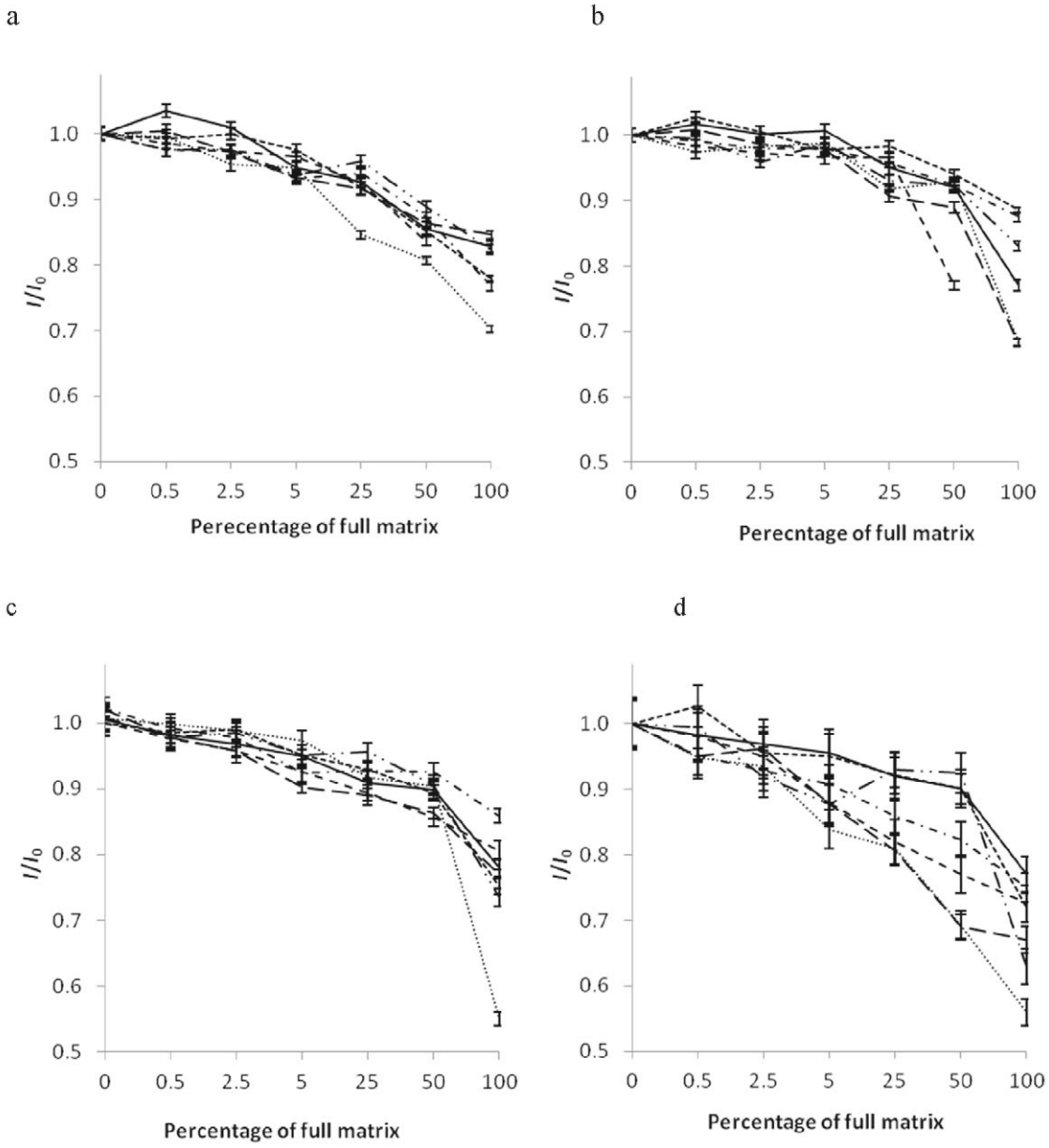

Fig. 3. Matrix effects for Cd(I) 228.802 nm for the tested sample introduction arrangements: (a) MMN+SC, (b) MMN+LC, (c) CCN+LC, (d) VGN+LC; ----- Na, —·— Ca, —··— Ba, ····· La, —— urea, ——— nitric acid, – – – all; CCN – concentric, MMN – Micromist, VGN – V-groove nebulizers, LC – large and SC – small spray chambers.

suppressive trend of Na, Ca and HNO_3 up to 50 % of an origin value on both the atomic and the ionic lines under robust conditions, whereas both suppression and enhancement (40–200 %) were observed under non-robust ones.

In our results, a specific trend in the matrix effect of EIEs (Na, Ca, Ba, La) was not detected, with the exception of La, which seems to cause the strongest signal decrease. Depending on the concentration of matrix, the single La effect is comparable or slightly stronger than that of mixed matrix, particularly at the highest concentrations of the matrix. Also Bauer and Broekaert (2007) did not find a clear difference in the intensity of the EIEs effects (Na, K, Rb and Ba). On the other hand, Chan & Hiftje (2008a) presented the order of EIEs influence decreasing to be: Na, Ca, Ba, La for ionic lines, while the bidirectional effect of La on atomic lines complicates the selection of internal standards. As well as in the presence of single La matrix, the lowest relative intensity and strong influence on the magnesium ionic-to-atomic intensity ratio (discussed below) were observed.

The matrix effects were observed in a wide range of matrix components concentrations. Figs. 3–10 reveal a strong dependence of relative intensities on the matrix concentration. Paredes et al. (2006) presented a continual decrease of relative intensities of 14 spectral lines in a wide range of increasing EIEs and or-

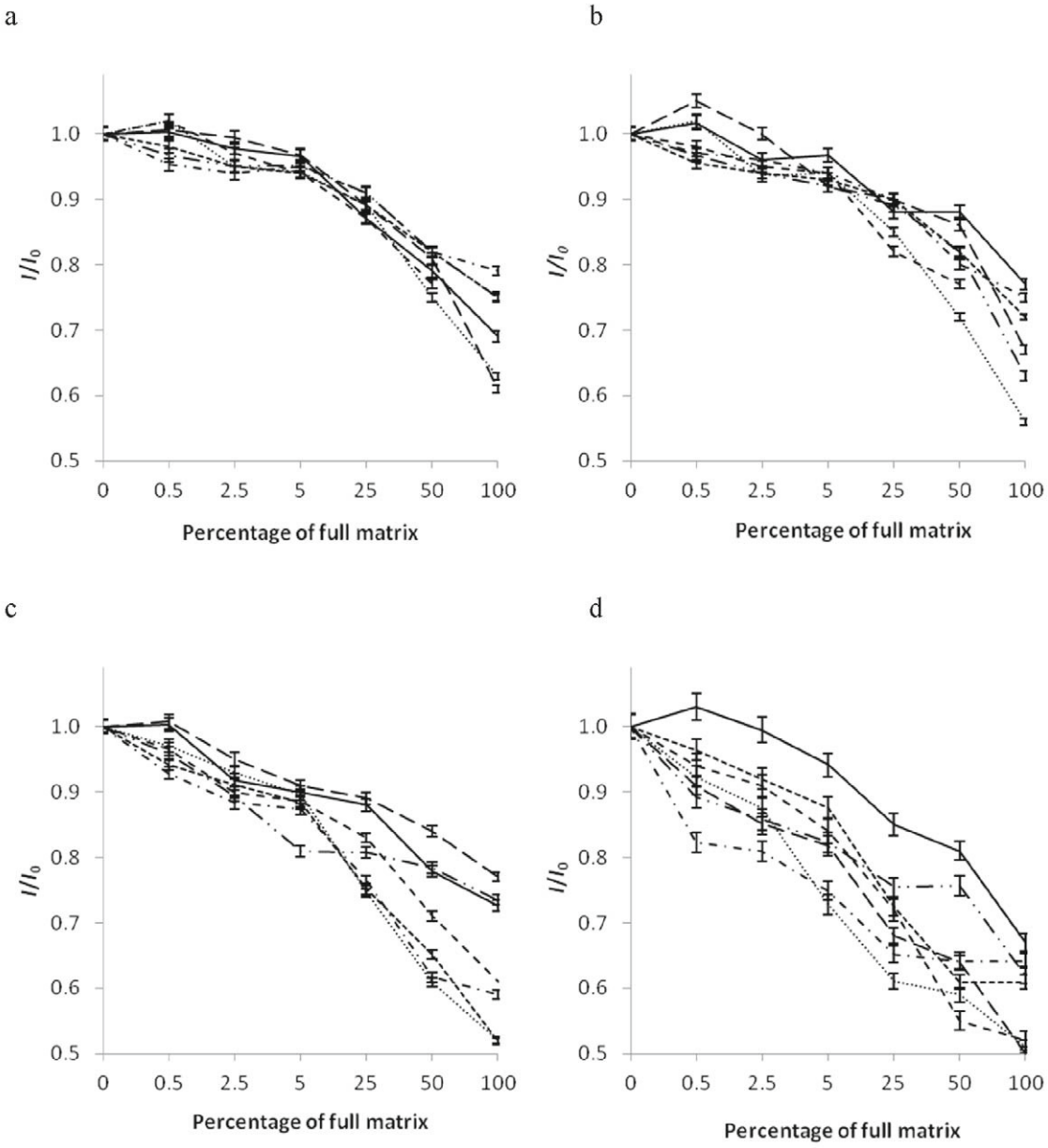

Fig. 4. Matrix effects for Cd(II) 214.438 nm for the tested sample introduction arrangements: (a) MMN+SC, (b) MMN+LC, (c) CCN+LC, (d) VGN+LC; (for legend explanation see Fig. 3).

ganic compounds concentrations. In our case, a similar trend was noticed. Initially, the relative intensity slowly decreases with the increasing matrix concentration and then, a sharper relative signal decline was observed. The concentration at which steeper decline can be observed depends on the sample introduction system employed; slightly higher matrix concentrations were determined for MMN compared to CCN and VGN. Across the studied spectral line and interferents in the "low" matrix (0.1 mass % of individual Na, Ca, Ba, La or urea, 10 vol. % of nitric acid or their mixture), the recoveries for both MMN arrangemnts were almost comparable: for the small volume spray chamber: 94–102 %, and for the large volume spray chamber: 91–101 %; a somewhat more significant difference between the results was originally expected. The CCN-LC arrangement revealed recoveries of 81–101 % and the VGN-LC one of 72–102 %. Recoveries for the "full matrix" (2 mass % of individual Na, Ca, Ba, La or urea, 20 vol. % of nitric acid or their mixture) obtained for all the instrumental arrangements were significantly worse (37–89 %) and they were mutually comparable. The "full" mixed matrix could not be analyzed using MMN as the nebulizer mouth was blocked. In terms of the recovery of the analysis, both MMN arrangements provided better results than the other nebulizers. Moreover, the I/I_0 values (I – intensity of signal for a model sample with matrix, I_0 – intensity of signal for a model sample with "zero" matrix) for the four sample introduction systems for the

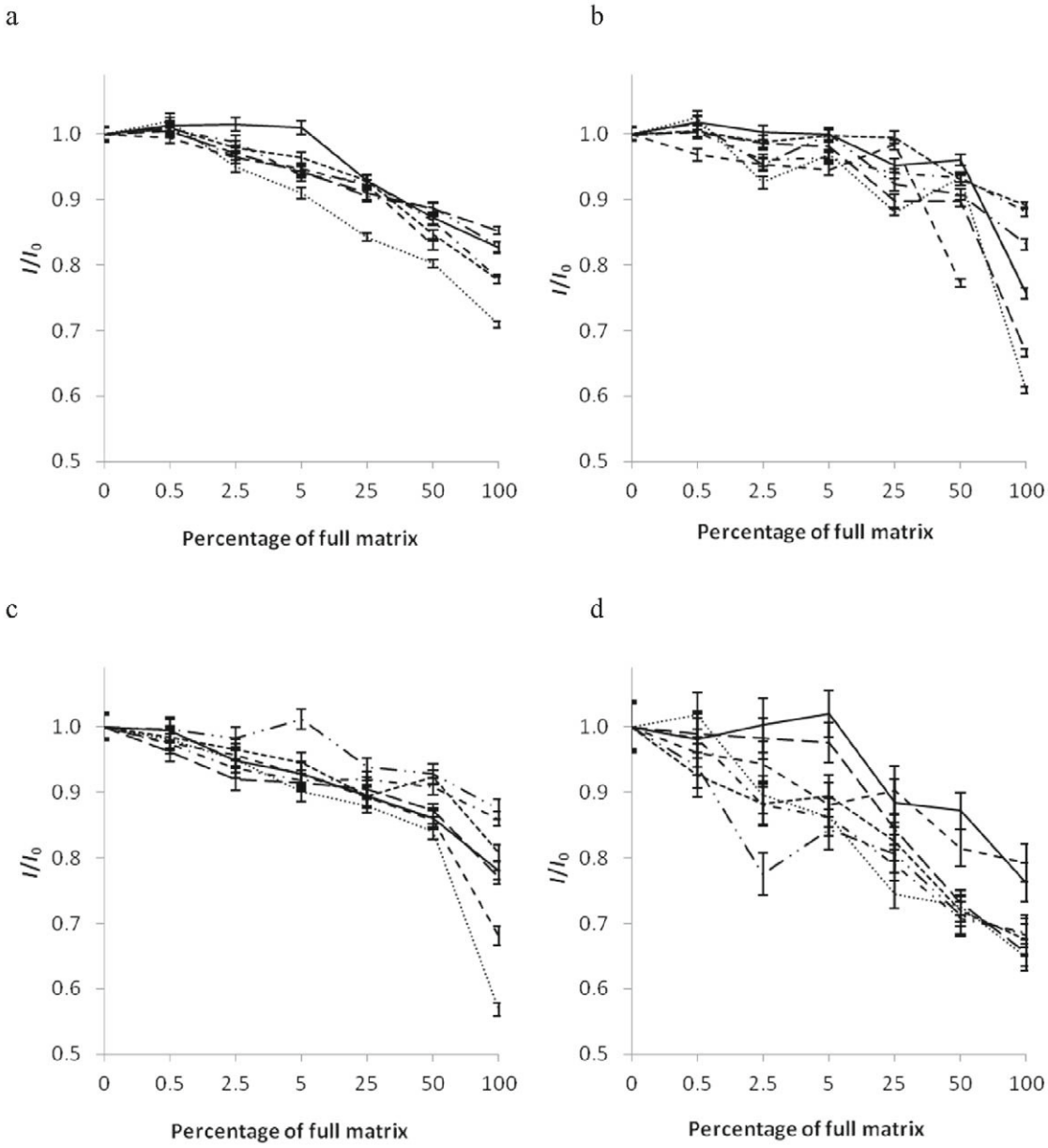

Fig. 5. Matrix effects for Cu(I) 324.754 nm for the tested sample introduction arrangements (a) MMN+SC, (b) MMN+LC, (c) CCN+LC, (d) VGN+LC; (for legend explanation see Fig. 3).

combined matrix (Table S2) revealed their dependence on the sample introduction set-up. From Figs. 3–10 follows that the combined effect is not a simple sum of the single effects (Todolí et al., 2004; Elgersma et al., 2000; Grotti et al., 2002).

Also, the influence of the sample uptake should be mentioned. For pneumatic nebulization, higher liquid flow led to an increased amount of the primary aerosol and the absolute number of small aerosol drops, which resulted in higher intensities (Vanhaecke et al., 1996). As it has been reported, the signal obtained in the presence of the matrix is less influenced at lower rates and an interval of rates where the matrix effects disappears can be found. On the other hand, the matrix effects caused by acids and, in a lower extent, by EIEs are more pronounced at low than at high liquid flow rates (Todolí et al., 1999, 2002, 2004; Elgersma et al., 2000). Maestre et al. (2002) found more intense matrix effects at low flow rates. According to the liquid flow rates typical for the microconcentric nebulizers presented in literature, our MMN flow rate was somewhat high and it seems to be from the opposite side as that in CCN operated at low liquid rates. At the CCN rates of 0.01–0.16 mL min^{-1} (Packer & Mattiazzo, 2007) and 0.05–0.2 mL min^{-1} (Elgersma et al., 2000), reduction of matrix effects was reported similarly in both MMN arrangements studied.

The final signal losses comprise probably more, even contradictory, effects. In our case, the observed matrix effects seem to be rather element/line inde-

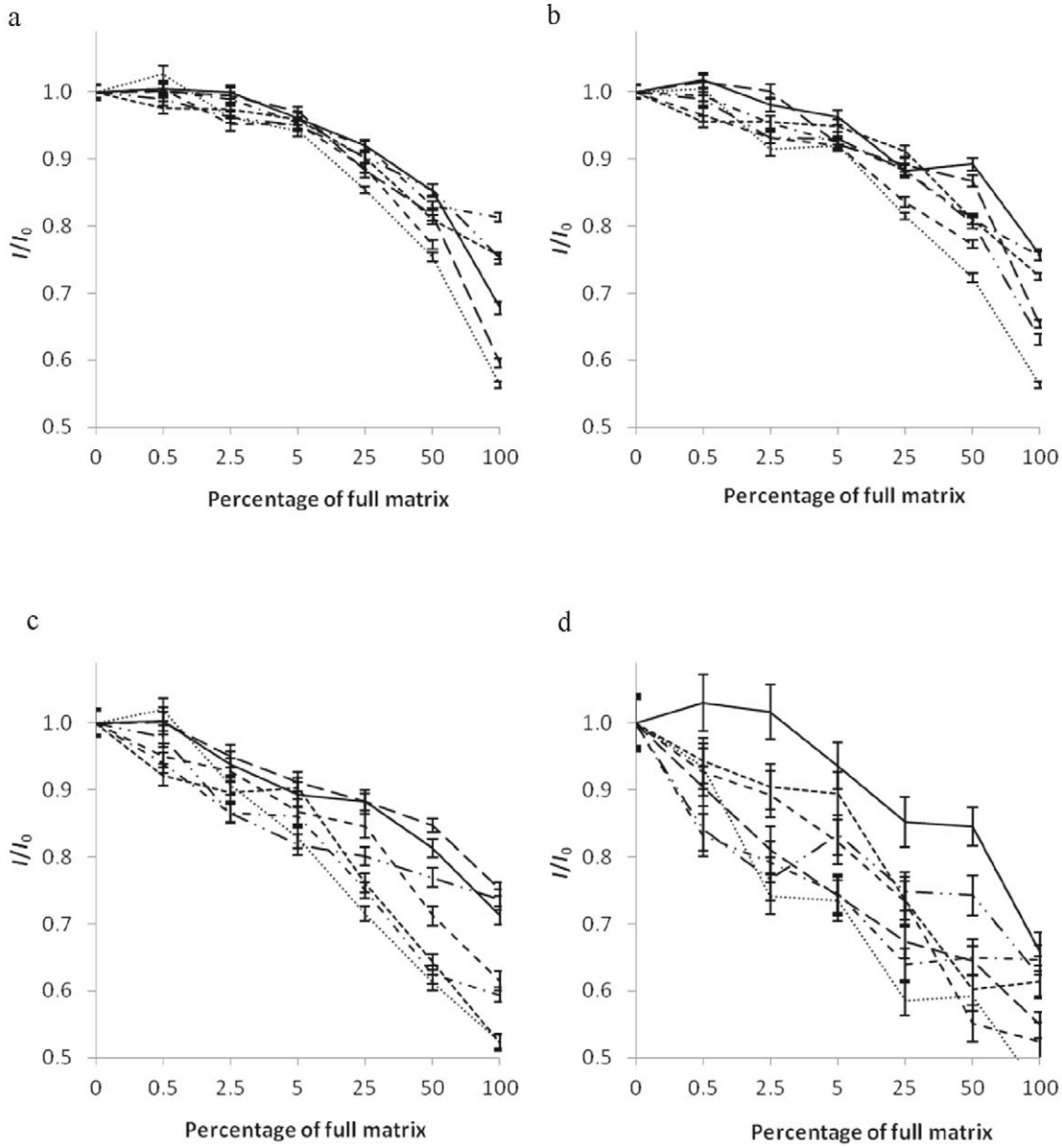

Fig. 6. Matrix effects for Cu(II) 224.700 nm for the tested sample introduction arrangements: (a) MMN+SC, (b) MMN+LC, (c) CCN+LC, (d) VGN+LC; (for legend explanation see Fig. 3).

pendent. Therefore, the phenomenon is likely to be more related to the changes in the transport behavior than to the plasma conditions (Todolí & Mermet, 2001). The decrease in signal intensities with the increasing matrix concentration can be also connected with processes inside the spray chamber which affect the tertiary aerosol. Inertial, gravitational, turbulence and centrifugal losses of larger and denser droplets within the spray chamber decrease the aerosol transport efficiency of the matrix containing solution compared to that of water. As reported, the aerosol leaving the spray chamber changes in the presence of matrix components compared to that obtained with pure water solutions due to the various solvent densities, deteriorated solvent evaporation and droplet formation (Canals et al., 1995; Todolí et al., 1999; Paredes et al., 2006). Efficiency of the sample transport in micronebulizers is in general far better than in common liquid sample introduction systems (Todolí & Mermet, 2001). Comparing all our LC arrangements, MMN revealed a slightly lower decrease in the signal intensity than CCN. MMN connected to LC provided slightly worse results compared to those obtained in SC, probably because of the not entirely geometrically suitable arrangement of these two components, which led to greater losses and worse efficiency of nebulization. MMN coupled with SC provided the best results. For a given set of nebulization conditions, the spray chamber role seems to be less significant than that of the nebulizer design.

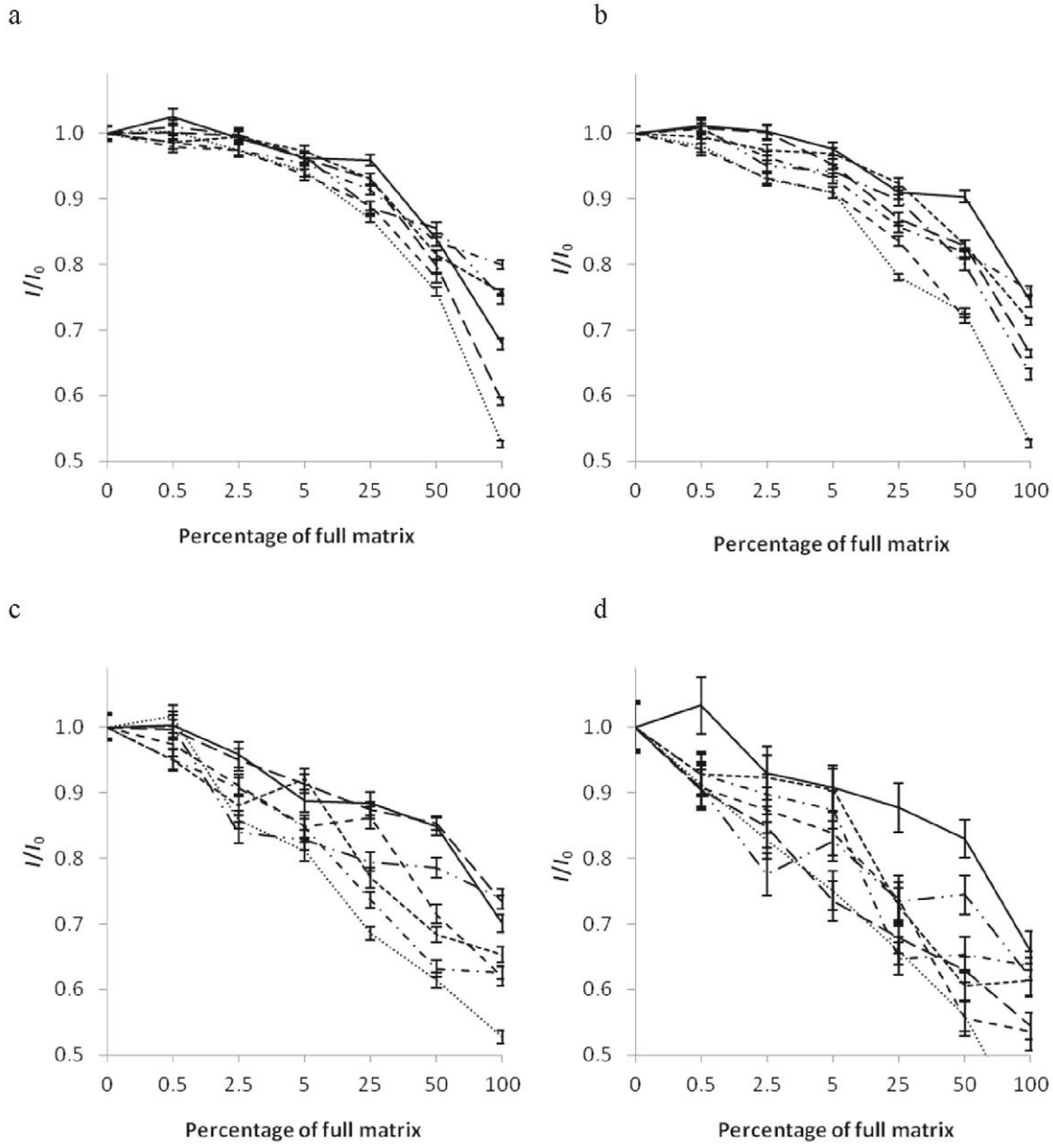

Fig. 7. Matrix effects for Mn II 257.610 nm for the tested sample introduction arrangements: (a) MMN+SC, (b) MMN+LC, (c) CCN+LC, (d) VGN+LC; (for legend explanation see Fig. 3).

Mg ionic-to-atomic (Mg(II)/Mg(I)) intensity ratios

Compared to the matrix free solution, the criterion of plasma robustness – magnesium ionic-to-atomic intensity ratio Mg(II) 280.270 nm/Mg(I) 285.213 nm (Mg(II)/Mg(I) ratio), is reduced if the interferences occur in plasma (Todolí et al., 2002; Stepan et al., 2001; Chan & Hieftje, 2008a; Bauer & Broekaert, 2007; Todolí & Mermet, 1999; Grotti et al., 2002; Rončević & Pitarević Svedružić, 2012). Variations in the Mg(II)/Mg(I) ratios in various matrices were determined (Table S3). With the exception of pure La matrix, the ratios were: 14–15, CCN 12–14.5, VGN 12.4–14.5 for both MMN arrangements and they slightly decreased as the matrix load increased indicating robust conditions. Todolí and Mermet (1999) attributed the matrix effects occurring under robust conditions to the aerosol generation and transport system which corresponds with our findings. More significant changes in the ratio were observed at the highest matrix concentration. When considering this ratio and the single intensities of Mg lines, the place where the matrix interferes could be revealed. In our case, this ratio did not change significantly but the signals of Mg lines did (as well as those of other spectral lines), which led to the assumption that the effect is rather element/line independent and more influenced by the sample transport (the sample introduction system

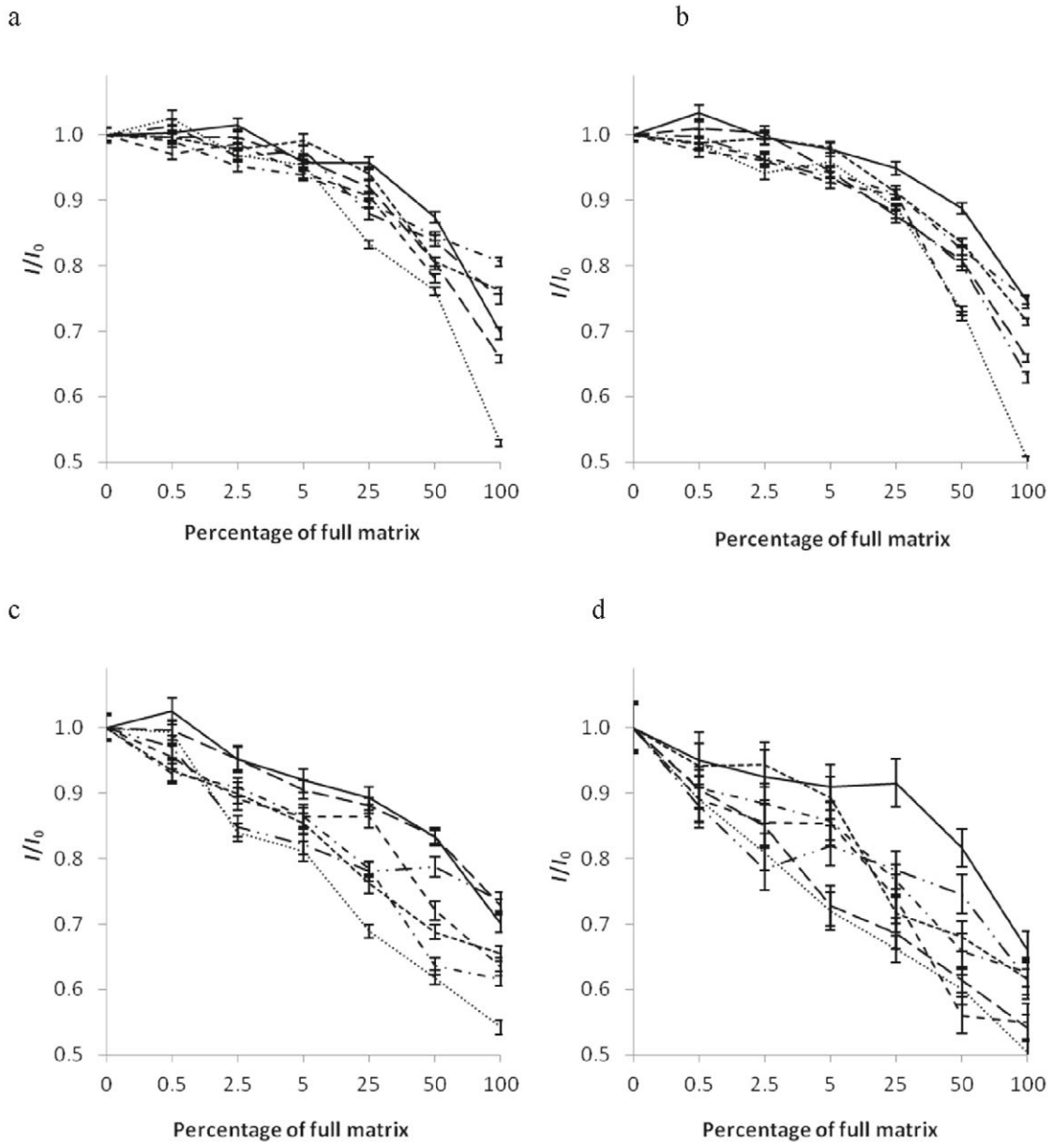

Fig. 8. Matrix effects for Pb(II) 220.353 nm for the tested sample introduction arrangements: (a) MMN+SC, (b) MMN+LC, (c) CCN+LC, (d) VGN+LC; (for legend explanation see Fig. 3).

used) than the plasma conditions (Todolí & Mermet, 2001).

Ratios of the mixed matrix were higher than those for pure La matrix. Model samples containing La revealed the strongest dependence on the matrix concentration, probably related to the shift of the excitation balance, which is consistent with Bauer and Broekaert (2007), who found that the plasma-related effects in the presence of EIEs are stronger (a decline in intensities) for ionic than for atomic spectral lines.

Conclusions

The study provides a board view of matrix effects and practical possibilities of reducing accompanying non-spectral interferences in ICP-OES using microconcentric Micromist nebulizers. The study deals with matrix effects and a wide scale of selected interferents in a wide concentration range and four sample introduction configurations. The matrix consisted of single Na, Ca, Ba, La, urea and HNO_3 and a mixture thereof up to 2 mass % of Na, Ca, Ba, La, urea and 20 vol. % of HNO_3 which is a wider range than reported previously. Concentric, V-groove and Micromist nebulizers were coupled with two cyclonic spray chambers of different sizes.

The presence of matrix strongly correlated with the decrease in the intensity (or analytical recoveries) of the analytical signal, more for ionic than for atomic spectral lines. LODs of "full" matrix were 1.6–

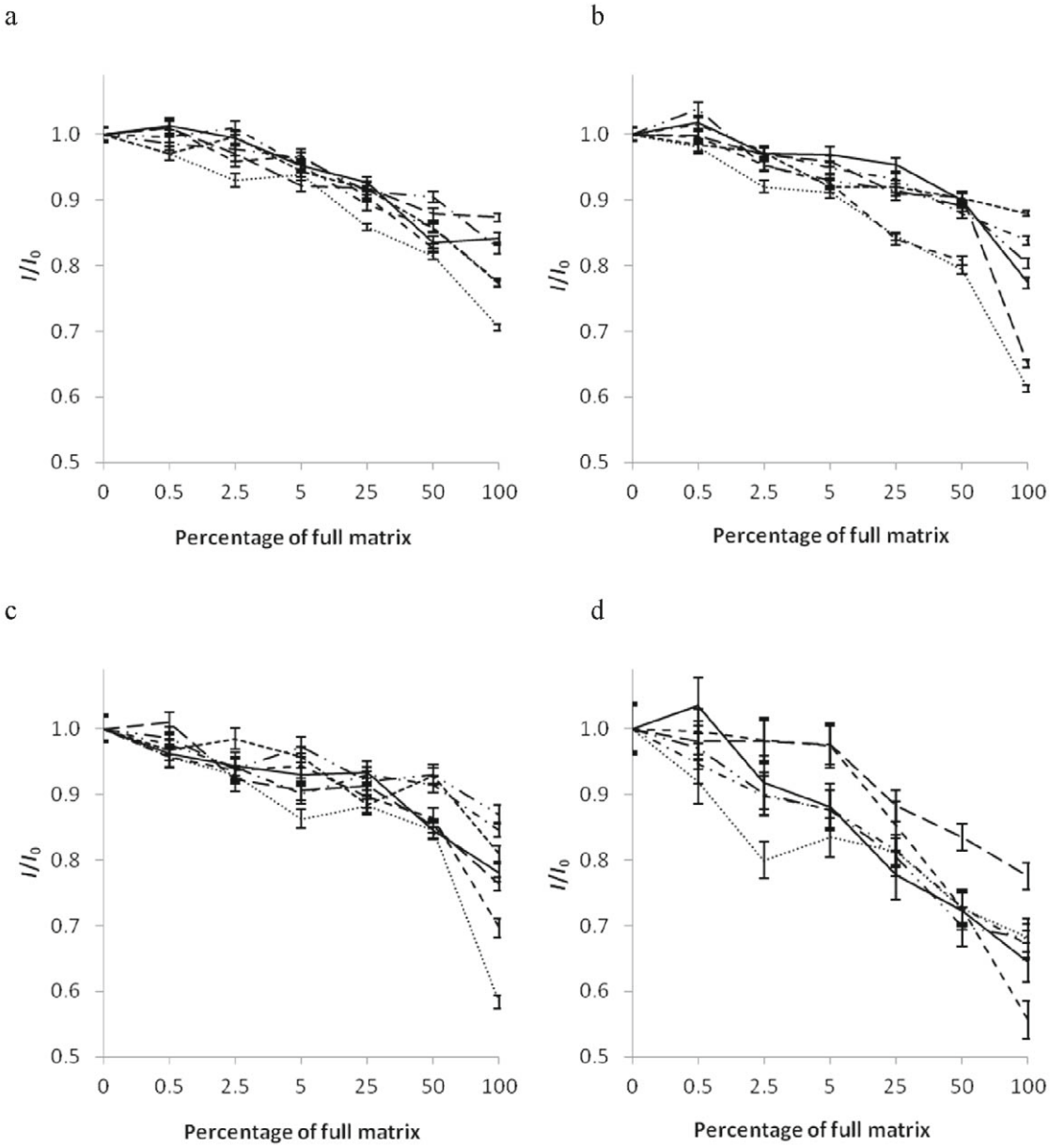

Fig. 9. Matrix effects for Zn(I) 213.856 nm for the tested sample introduction arrangements: (a) MMN+SC, (b) MMN+LC, (c) CCN+LC, (d) VGN+LC; (for legend explanation see Fig. 3).

2.1 times higher than for the "zero" one and they were slightly higher for ionic than for the atomic lines. Also, slightly higher CVs were obtained for the "full" matrix than for the "zero" one. The Mg(II)/Mg(I) ratios of 12–15 indicated that the process was operated under robust conditions. The ratios decreased negligibly with the increasing matrix load. Pure La matrix showed the steepest decline in the Mg(II)/Mg(I) ratio, probably due to the shift in the excitation balance, even steeper than that observed for the mixed matrix. This led to the assumption that the transport interferences affecting the tertiary aerosol outweighed the plasma related effect for the mixed matrix.

For the "low" matrix, the obtained relative intensities were 94–102 % for the MMN-SC and 91–101 % for the MMN-LC arrangement, while they were 81–101 % for CCN-LC and 72–102 % for VGN-LC. Recoveries for the extremely "full" matrix were significantly worse, 37–85 %, for all the arrangements. The Mg(II)/Mg(I) ratios were very similar for both MMN arrangements: 14–15, 12–14.5 for CCN, and 12.4–14.5 for VGN 5.

Compared to other nebulizer arrangements, MMC-SC revealed the lowest matrix effects across the range of matrix loads and exhibited evidently the least significant dependence without worsening the analytical characteristics. Liquid flow rate in this arrangement was somewhere like a "grey" zone. The MMN flow rate employed was somewhat high, comparable with that in CCN operated at low flow rates. According

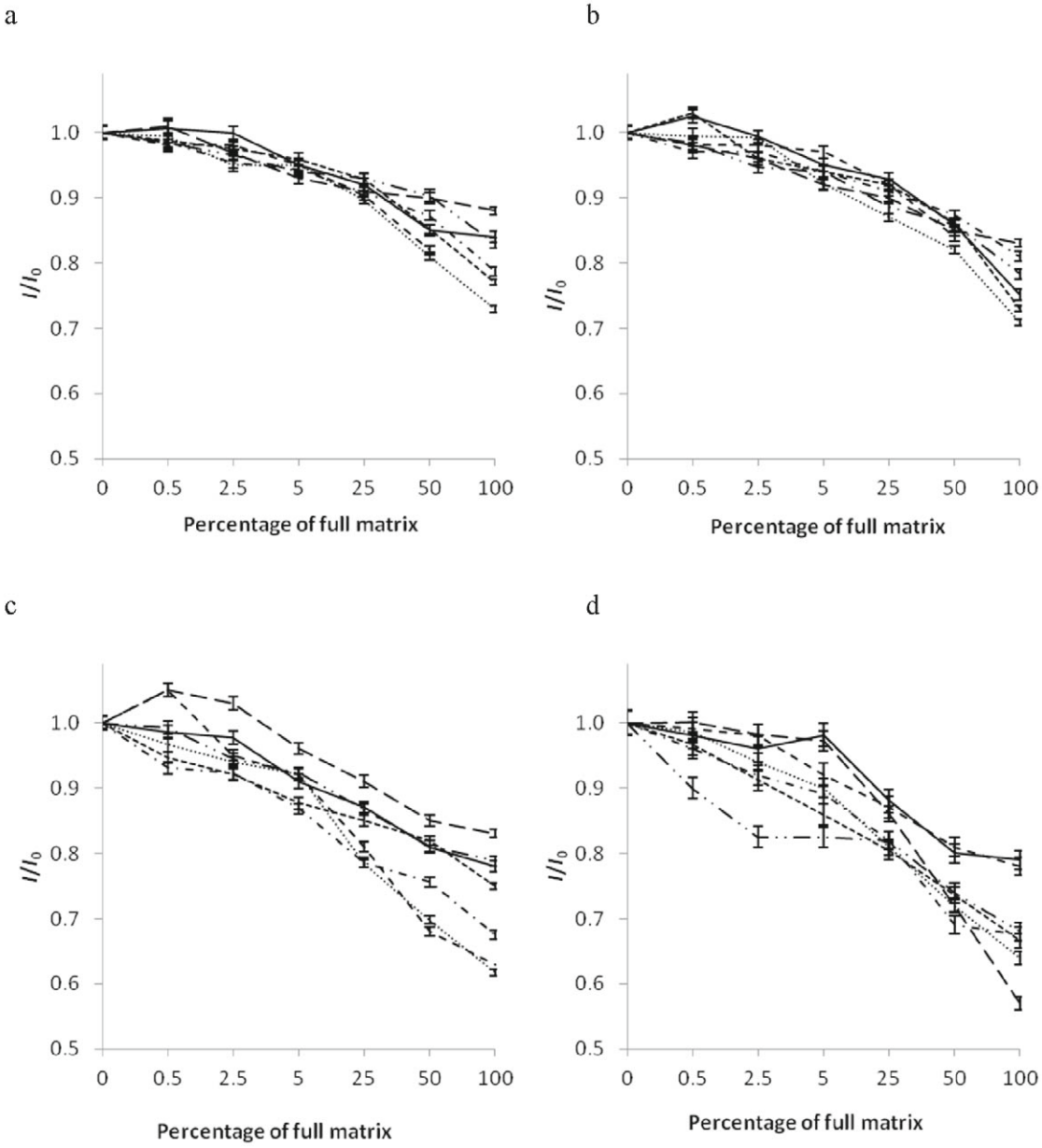

Fig. 10. Matrix effects for K(I) 766.490 nm for the tested sample introduction arrangements: (a) MMN+SC, (b) MMN+LC, (c) CCN+LC, (d) VGN+LC; (for legend explanation see Fig. 3).

to the results obtained, this MMN-SC arrangement provides an analytical method as independent on the matrix effects as possible and enables reducing the consumption of the sample compared to the conventional arrangement to approximately a half.

Acknowledgements. he authors are grateful to the SG FCHT 05/2015 project for financial support.

Supplementary data

Supplementary data associated with this article can be found in the online version of this paper (DOI: 10.1515/chempap-2016-0004).

References

Aguirre, M. Á., Kovachov, N., Almagro, B., Hidalgo, M., & Canals, A. (2010). Compensation for matrix effects on ICP-OES by on-line calibration methods using a new multi-nebulizer based on Flow Blurring®technology. *Journal of Analytical Atomic Spectrometry*, *25*, 1724–1732. DOI: 10.1039/c004854b.

Ardini, F., Grotti, M., Sánchez, R., & Todolí, J. L. (2012). Improving the analytical performances of ICP-AES by using a high-temperature single-pass spray chamber and segmented-injections micro-sample introduction for the analysis of environmental samples. *Journal of Analytical Atomic Spectrometry*, *27*, 1400–1404. DOI: 10.1039/c2ja30152k.

Bauer, M., & Broekaert, J. A. C. (2007). Investigations on the use of pneumatic cross-flow nebulizers with dual solu-

tion loading including the correction of matrix effects in elemental determinations by inductively coupled plasma optical emission spectrometry. *Spectrochimica Acta Part B: Atomic Spectroscopy*, *62*, 145–154. DOI: 10.1016/j.sab.2007.02.006.

Becker, J. S., & Dietze, H. J. (1999). Ultratrace and isotope analysis of long-lived radionuclides by inductively coupled plasma quadrupole mass spectrometry using a direct injection high efficiency nebulizer. *Analytical Chemistry*, *71*, 3077–3084. DOI: 10.1021/ac9900883.

Benzo, Z., Maldonado, D., Chirinos, J., Marcano, E., Gómez, C., Quintal, M., & Salas, J. (2009). Evaluation of dual sample introduction systems by comparison of cyclonic spray chambers with different entrance angles for ICP-OES. *Microchemical Journal*, *93*, 127–132. DOI: 10.1016/j.microc.2009.05.009.

Borkowska-Burnecka, J., Leśniewicz, A., & Żyrnicki, W. (2006). Comparison of pneumatic and ultrasonic nebulizations in inductively coupled plasma atomic emission spectrometry – matrix effects and plasma parameters. *Spectrochimica Acta Part B: Atomic Spectroscopy*, *61*, 579–587. DOI: 10.1016/j.sab.2006.04.005.

Canals, A., Hernandis, V., Todoli, J. L., & Browner, R. F. (1995). Fundamental studies on pneumatic generation and aerosol transport in atomic spectrometry: effect of mineral acids on emission intensity in inductively coupled plasma atomic emission spectrometry. *Spectrochimica Acta Part B: Atomic Spectroscopy*, *50*, 305–321. DOI: 10.1016/0584-8547(94)00138-l.

Cano, J. M., Todolí, J. L., Hernandis, V., & Mora, J. (2002). The role of the nebulizer on the sodium interferent effects in inductively coupled plasma atomic emission spectrometry. *Journal of Analytical Atomic Spectrometry*, *17*, 57–63. DOI: 10.1039/b105077j.

Chan, G. C. Y., & Hieftje, G. M. (2008a). Warning indicators for the presence of plasma-related matrix effects in inductively coupled plasma-atomic emission spectrometry. *Journal of Analytical Atomic Spectrometry*, *23*, 181–192. DOI: 10.1039/b706837a.

Chan, G. C. Y., & Hieftje, G. M. (2008b). Use of vertically resolved plasma emission as an indicator for flagging matrix effects and system drift in inductively coupled plasma-atomic emission spectrometry. *Journal of Analytical Atomic Spectrometry*, *23*, 193–204. DOI: 10.1039/b706838g.

de Gois, J. S., Maranhão, T. D. A., Oliveira, F. J. S., Frescura, V. L. A., Curtius, A. J., & Borges, D. L. G. (2012). Analytical evaluation of nebulizers for the introduction of acetic acid extracts aiming at the determination of trace elements by inductively coupled plasma mass spectrometry. *Spectrochimica Acta Part B: Atomic Spectroscopy*, *77*, 35–43. DOI: 10.1016/j.sab.2012.08.001.

Dubuisson, C., Poussel, E., Todolí, J. L., & Mermet, J. M. (1998). Effect of sodium during the aerosol transport and filtering in inductively coupled plasma atomic emission spectrometry. *Spectrochimica Acta Part B: Atomic Spectroscopy*, *53*, 593–600. DOI: 10.1016/s0584-8547(98)00084-6.

Elgersma, J. W., Thuy, D. T., & Groenestein, R. P. (2000). Efficient use of a conventional pneumatic concentric nebulizer in ICP-AES at low liquid uptake rates by applying a desolvation system: determination of detection limits and degrees of acid interferences. *Journal of Analytical Atomic Spectrometry*, *15*, 959–966. DOI: 10.1039/b003250f.

Grotti, M., Leardi, R., & Frache, R. (2002). Combined effects of inorganic acids in inductively coupled plasma optical emission spectrometry. *Spectrochimica Acta Part B: Atomic Spectroscopy*, *57*, 1915–1924. DOI: 10.1016/s0584-8547(02)00161-1.

Iglésias, M., Vaculovic, T., Studynkova, J., Poussel, E., & Mermet, J. M. (2004). Influence of the operating conditions and of the optical transition on non-spectral matrix effects in inductively coupled plasma-atomic emission spectrometry. *Spectrochimica Acta Part B: Atomic Spectroscopy*, *59*, 1841–1850. DOI: 10.1016/j.sab.2004.09.007.

Krejčová, A., Černohorský, T., & Čurdová, E. (2001). Determination of sodium, potassium, magnesium and calcium in urine by inductively coupled plasma atomic emission spectrometry. The study of matrix effects. *Journal of Analytical Atomic Spectrometry*, *16*, 1002–1005. DOI: 10.1039/b101941o.

Krejčová, A., & Černohorský, T. (2003). Comparision of methods used for elimination of matrix effect in ICP-AES. *Scientific Papers of the University of Pardubice series A*, 173–186.

Lehn, S. A., Warner, K. A., Huang, M., & Hieftje, G. M. (2003). Effect of sample matrix on the fundamental properties of the inductively coupled plasma. *Spectrochimica Acta Part B: Atomic Spectroscopy*, *58*, 1785–1806. DOI: 10.1016/s0584-8547(03)00159-9.

Lide, D. R. (2003). *CRC handbook of chemistry and physics. Section 10: Atomic, molecular, and optical physics; ionization potentials of atoms and atomic ions* (84th ed.). Boca Raton, FL, USA: CRC Press.

Maestre, S., Mora, J., & Todolí, J. L. (2002). Studies about the origin of the non-spectroscopic interferences caused by sodium and calcium in inductively coupled plasma atomic emission spectrometry. Influence of the spray chamber design. *Spectrochimica Acta Part B: Atomic Spectroscopy*, *57*, 1753–1770. DOI: 10.1016/s0584-8547(02)00141-6.

Maestre, S. E., Todolí, J. L., & Mermet, J. M. (2004). Evaluation of several pneumatic micronebulizers with different designs for use in ICP–AES and ICP–MS. Future directions for further improvement. *Analytical and Bioanalytical Chemistry*, *379*, 888–899. DOI: 10.1007/s00216-004-2664-4.

Matusiewicz, H., Ślachciński, M., Hidalgo, M., & Canals, A. (2007). Evaluation of various nebulizers for use in microwave induced plasma optical emission spectrometry. *Journal of Analytical Atomic Spectrometry*, *22*, 1174–1178. DOI: 10.1039/b704612j.

Mora, J., Maestre, S., Hernandis, V., & Todolí, J. L. (2003). Liquid-sample introduction in plasma spectrometry. *Trends in Analytical Chemistry*, *22*, 123–131. DOI: 10.1016/s0165-9936(03)00301-7.

Packer, A. P., & Mattiazzo, M. E. (2007). Influence of organic and inorganic acids commonly used in soil extraction and digestion procedures in the determination of elements by inductively coupled plasma optical emission spectrometry. *Atomic Spectroscopy*, *28*, 129–136.

Paredes, E., Maestre, S. E., & Todolí, J. L. (2006). Use of stirred tanks for studying matrix effects caused by inorganic acids, easily ionized elements and organic solvents in inductively coupled plasma atomic emission spectrometry. *Spectrochimica Acta Part B: Atomic Spectroscopy*, *61*, 326–339. DOI: 10.1016/j.sab.2006.03.005.

Rončević, S., & Pitarević Svedružić, L. (2012). Evaluation of matrix effects of polycarboxylic acid introduction in inductively coupled plasma atomic emission spectrometry (ICP-AES). *Croatica Chemica Acta*, *85*, 311–317. DOI: 10.5562/cca2066.

Silva, F. V., Trevizan, L. C., Silva, C. S., Nogueira, A. R. A., & Nóbrega, J. A. (2002). Evaluation of inductively coupled plasma optical emission spectrometers with axially and radially viewed configurations. *Spectrochimica Acta Part B: Atomic Spectroscopy*, *57*, 1905–1913. DOI: 10.1016/s0584-8547(02)00176-3.

Stepan, M., Musil, P., Poussel, E., & Mermet, J. M. (2001). Matrix-induced shift effects in axially viewed inductively coupled plasma atomic emission spectrometry. *Spectrochim-*

ica Acta Part B: Atomic Spectroscopy, *56*, 443–453. DOI: 10.1016/s0584-8547(01)00171-9.

Stewart, I. I., & Olesik, J. W. (1998). Steady state acid effects in ICP-MS. *Journal of Analytical Atomic Spectrometry*, *13*, 1313–1320. DOI: 10.1039/a806040a.

Todolí, J. L., & Mermet, J. M. (1999). Acid interferences in atomic spectrometry: analyte signal effects and subsequent reduction. *Spectrochimica Acta Part B: Atomic Spectroscopy*, *54*, 895–929. DOI: 10.1016/s0584-8547(99)00041-5.

Todolí, J. L., Hernandis, V., Canals, A., & Mermet, J. M. (1999). Comparison of characteristics and limits of detection of pneumatic micronebulizers and a conventional nebulizer operating at low uptake rates in ICP-AES. *Journal of Analytical Atomic Spectrometry*, *14*, 1289–1295. DOI: 10.1039/a900598f.

Todolí, J. S., & Mermet, J. M. (2001). Evaluation of a direct injection high-efficiency nebulizer (DIHEN) by comparison with a high-efficiency nebulizer (HEN) coupled to a cyclonic spry chamber as a liwuid sample introduction system for ICP-AES. *Journal of Analytical Atomic Spectrometry*, *16*, 514–520. DOI: 10.1039/b009430g.

Todolí, J. L., Gras, L., Hernandis, V., & Mora, J. (2002). Elemental matrix effects in ICP-AES. *Journal of Analytical Atomic Spectrometry*, *17*, 142–169. DOI: 10.1039/b009570m.

Todolí, J. L., Maestre, S. E., & Mermet, J. M. (2004). Compensation for matrix effects in ICP-AES by using air segmented liquid microsample introduction. The role of the spray chamber. *Journal of Analytical Atomic Spectrometry*, *19*, 728–737. DOI: 10.1039/b317082a.

Tripković, M. R., & Holclajtner-Antunović, I. D. (1993). Study of the matrix effect of easily and non-easily ionizable elements in an inductively coupled argon plasma. Part 1. Spectroscopic diagnostics. *Journal of Analytical Atomic Spectrometry*, *8*, 349–357. DOI: 10.1039/ja9930800349.

Vanhaecke, F., van Holderbeke, M., Moens, L., & Dams, R. (1996). Evaluation of a commercially available microconcentric nebulizer for inductively coupled plasma mass spectrometry. *Journal of Analytical Atomic Spectrometry*, *11*, 543–548. DOI: 10.1039/ja9961100543.